J Mater Sci (2011) 46:5221–5226
DOI 10.1007/s10853-011-5459-y

Electrochemical deposition and magnetic properties of cobalt and iron thin films on substrate of KIT-6/ITO

Tingting Gao · Guangbin Ji · Xiaofeng Chang · Xiaohui Lin · Jinsong Liu · M. Qamar

Received: 2 December 2010 / Accepted: 9 March 2011 / Published online: 23 March 2011

Abstract Cobalt and iron thin films were successfully electrodeposited on the KIT-6/ITO substrate. The films consisted of mesoporous structure (the average pore size of which was estimated at ~5 nm) and large specific surface area (431 m^2/g). The nanofilms were further characterized by X-ray diffractometer, scanning electron microscope, and vibrating sample magnetometer. The results indicated that the Fe magnetic films tend to grow preferentially along Fe (002) crystal direction while the Co film grew along both (101) and (220) crystal directions. The as-obtained magnetic metal films exhibited ferromagnetic behavior and both the values of coercivities parallel to the films were examined below 50 Oe.

Introduction

It is now generally accepted that the control of material's architecture at nanoscale could lead to the development of new materials and systems with promising physical and chemical properties owing to their reduced size and increased surface area. The success lies in the appropriate tailoring and engineering of the nanomaterials and their resulting devices for a given application [1, 2]. The memory density of devices can be greatly improved by fabricating magnetic materials in nanostructured forms [3, 4]. Considerable amount of scientific research have been directed toward the development of magnetic and optical storage components with critical dimensions as small as tens of nanometers [3–5]. Recently, devices made of magnetic nanofilms with high magnetoresistance have attracted much attention due to its potential application in information technology sector. Due to their improved properties such as anisotropic magnetoresistance, single crystalline ferromagnetic films of transition metals, such as Ni, Fe, Co, and their alloys have been applied in radio-frequency integrated circuits [5, 6].

A number of methodologies have been developed in recent past years to fabricate and design nanostructured materials [7–8]. Recently, the development of nanostructured materials with mesoporosity has received particular attention owing to the high specific surface area and porosity which are expected to boost the activity of materials toward a wide variety of reactions. In this regard, mesoporous inorganic structures have been applied, due to highly ordered nanochannels, as a building block for the development of tailored nanomaterials [9]. KIT-6, a kind of three-dimensional bicontinuous cubic *Ia3d* mesoporous material with highly ordered hexagonally arranged mesochannels, thick walls, adjustable pore size from 3 to 30 nm and high hydrothermal/thermal stability [10] has been widely used for the synthesis of different semiconductor oxides such as CeO_2 and WO_3 [11] and organometallic catalysts such as Ru-PPh2-KIT-6 [12]. Sol–gel processing is very suitable for the preparation of such nanocomposites as it offers unique advantages in terms of compositional homogeneity, dispersion of the nanophase within the matrix and purity of the resulting material [13, 14]. Park et al. [15] reported the preparation of mesoporous silica

T. Gao · G. Ji (✉) · X. Chang · X. Lin · J. Liu
Department of Applied Chemistry, College of Materials Science and Technology, Nanjing University of Aeronautics and Astronautics, Nanjing 211100, People's Republic of China
e-mail: gbji@nuaa.edu.cn

M. Qamar
Center of Excellence in Nanotechnology (CENT), King Fahd University of Petroleum and Minerals, Dhahran 31261, Saudi Arabia

(MS) film with thickness of 400 nm using F127 as an organic template surfactant through a spin coating process .

Electrochemical process has also been considered as an effective approach for depositing metals crystals into the pores of nanoscale templates (such as alumina membranes, nuclear track-etched polymer membranes, MS, or porous silicon) in order to obtain unique property [16, 17] due to it's advantages such as simple, low-cost, and high-throughput.

In this study, KIT-6 was synthesized and used as a building block for the growth of Co and Fe thin films. KIT-6 was deposited on ITO substrate using spin coating technique while thin films of Co and Fe were grown following electrochemical deposition method. Various properties such as porestructure, microstructure, and magnetic properties of nanofilms were investigated by means of N_2 adsorption–desorption measurement, X-ray diffractometer (XRD), scanning electron microscope (SEM), and vibrating sample magnetometer (VSM).

Experiment

Preparation of KIT-6 precursor and KIT-6/ITO substrate

The KIT-6 precursor was prepared using Pluronic P123 (EO20-PO70-EO20, MW = 5800, Aldrich) as a structure-directing agent and tetraethyl orthosilicate (TEOS) (Aldrich, 98%) as the silica precursor according to the published literature [18, 19]. In brief, 4.0 g of P123 was dissolved in 144-mL distilled water followed by addition of 7.9 g of 35 wt% HCl solution with stirring at 35 °C. After complete dissolution, 4.0 g of *n*-butanol (BuOH) was added and the solution was stirred for 1 h. The KIT-6 precursor was obtained by adding 8.6 g of TEOS to the homogeneous clear solution followed by stirring for another 1 h. The preparation process was carried out in a closed polypropylene bottle.

The ITO/KIT-6 substrate was obtained by the following steps. First, the substrate was rinsed with distilled water and cleaned with acetone and alcohol under ultrasonic treatment for 20 min and was dried in the air. The dried substrate was then put on the spin coating machine under the vacuum and the machine was adjusted as the low speed of 500 r/min for 18 s and the high speed of 1500 r/min for 40 s. The KIT-6 precursor was dropped on the substrate during the low speed and the film was spread uniformly at the high speed. The resulting film was aged at 100 °C for 12 h followed by calcination at 400 °C for 1 h (with a heating speed of 1 °C/min) to remove the polymer template.

The electrodeposition of nanofilm

The procedure describing the fabrication of KIT-6 followed by Co and Fe films on ITO substrate is schematically shown in Fig. 1. For electrodeposition of Co and Fe nanofilm, direct current, carbon rods, and the substrate were used. The electrolyte solution was composed of $FeSO_4$, H_3BO_3, and the ascorbic acid (VC). The KIT-6 has a structure of three-dimensional bicontinuous cubic *Ia3d* mesochannels whose one side is open while the other is closed with the glass. Therefore, the electrodeposition occurred from the conductive surface of ITO and along the mesochannels. The film was found to be composed of a number of nanowires which has been reported earlier [19–21].

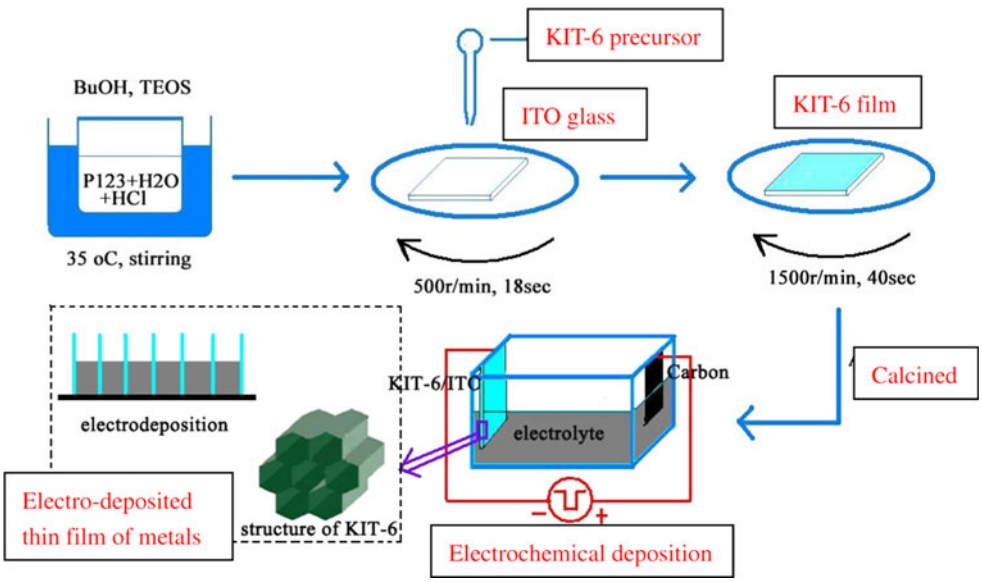

Fig. 1 Schematic representation of the procedure used for the fabrication of KIT-6 and Co, Fe films on the ITO substrate

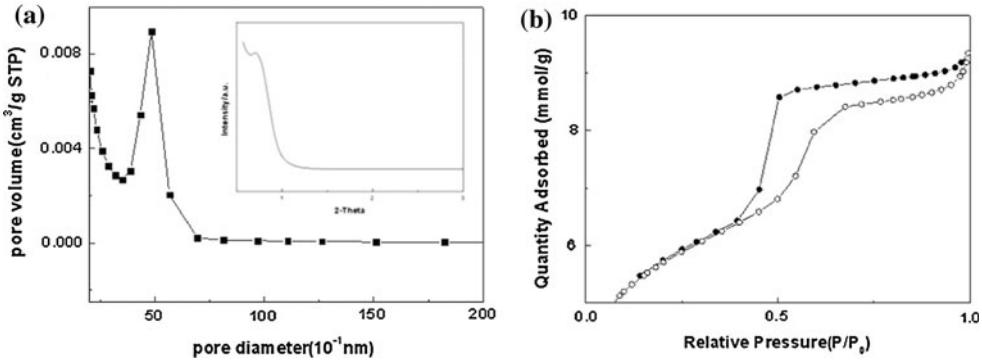

Fig. 2 (**a**) Pore size distribution and (**b**) Nitrogen adsorption–desorption isotherms by BHJ method for the KIT-6 (inset of (**a**) shows the corresponding SAXRD)

The pore structure of as-prepared KIT-6 silica template was studied by N_2 adsorption–desorption isotherm (at 77 K) which was measured by a Micromeritics ASAP 2020 gas sorption system. The morphology of as-prepared samples was investigated by means of SEM (JEOL S4800) and TEM (JEOL JEM 2100). The crystal structure and the texture of the KIT-6 silica template and nanofilms with ITO were studied by XRD (Bruker D8 ADVANCE) and the magnetic properties of Co and Fe films at room temperature were measured by VSM (Lake shore 7410).

Results and discussion

As shown in Fig. 2a, the average pore size, obtained by a Barrett–Joyner–Halenda (BHJ) analysis, for the mesoporous sample is centered at $\sim$5.0 nm. The surface area, pore size, and pore volume of KIT-6 support were investigated by the nitrogen adsorption/desorption isotherms. The pore volume and specific surface area, obtained by the BET method, of mesoporous KIT-6 were found to be 0.32 $cm^3\ g^{-1}$ and 431 m^2/g, respectively [22]. It was noticed that both the values, estimated in the study, are larger than that of previously reported [23], which might be attributed to the correlation of lower pore volume and smaller diameter. The inset figure depicts the small angle X-ray diffraction (SAXRD) pattern of KIT-6 films on ITO and 1 weak diffraction peak can be observed at $2\theta = 0.5°$, possibly caused by the incident peak of X-ray. Surprisingly, the characteristic diffraction peak of KIT-6 which appears at 2θ of 1° could not be observed which implies that the as-prepared KIT-6 nanofilm is not long-range ordered structure. This may be collectively attributed to the external forces such as surface tension between precursor and the glass, centrifugal force, calcination environment, and so on which could possibly destroy the ordered structure of KIT-6 structure [24].

The N_2 adsorption–desorption isotherms of KIT-6 shown in Fig. 1b suggested a representative type IV characteristic of as-prepared KIT-6, exhibiting a well-defined step for the relative pressure P/P_0 ranging from 0.4 to 0.6 which is the characteristic of mesoporous materials. The delayed close of adsorption and desorption isotherms may be caused by the mass of microporous structure according to Fig. 2a.

The microstructural and morphological properties of as-prepared KIT-6 nanolayers was further explored by TEM after separating nanolayers from the ITO glass. Figure 3 depicts the mesoporous structure and a mean diameter of

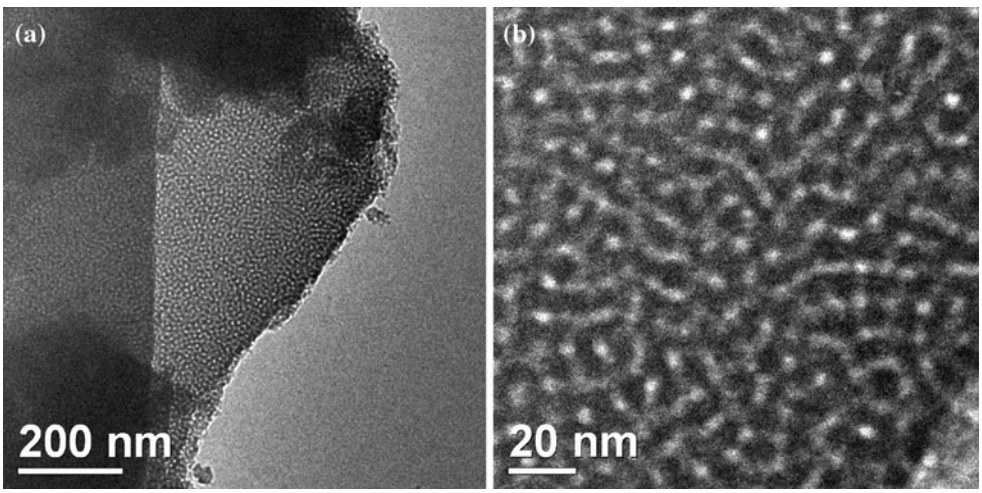

Fig. 3 Representative TEM images of KIT-6 nanolayers separated from ITO glass

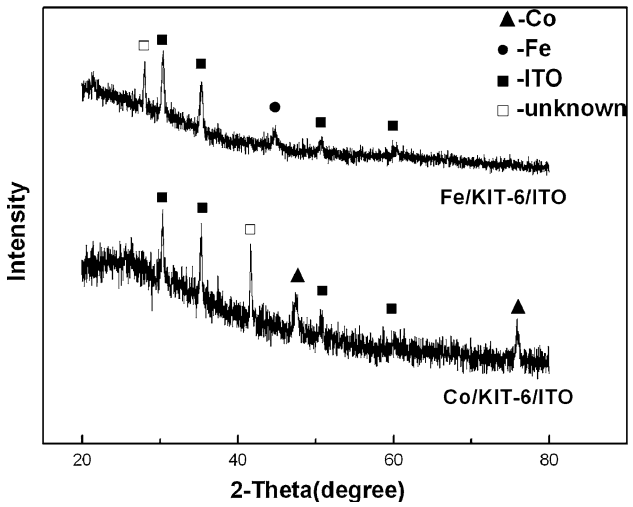

Fig. 4 XRD patterns of Fe/KIT-6/ITO and Co/KIT-6/ITO

about 4–5 nm of the sample which is consistent with the pore structure analysis. The disordered arrangement of the pore channels was observed to irregular which was in agreement with the SAXRD result.

To overcome the surface tension and insure the uniform distribution of the membrane and avoid the different thickness range from the template, the machine with low and high rotational speed was used. The precursor was dropped on the ITO at the low speed 500 r/min, and the mesochannels were arranged at the high speed 1500 r/min for 50 s. Under the high speed, the mesochannel will be bent and, in addition, a high temperature treatment inevitably causes the mesostructure to distort to some extent.

Figure 4 shows the wide angle X-ray diffraction patterns of ITO/KIT-6/Fe and ITO/KIT-6/Co samples. As the KIT-6/Fe and KIT-6/Co can not be separated from the ITO glass easily, the XRD patterns of the samples were measured along with ITO/KIT-6 substrate and the diffraction peaks were marked. A weak diffraction peak corresponding to the (110) plane of Fe crystal was found at 2θ of 44.66° as presented in Fig. 4 indicating that the as-deposited Fe particles on the template grew preferentially along Fe (002) crystal direction. Moreover, the diffraction peaks corresponding to the (101) and (220) planes of Co crystal were also detected at 2θ of 47.43° and 75.85°,respectively. However, the extra peak appeared at $2\theta = 28.05°$ in ITO/KIT-6/Fe might be attributed to the cathodic corrosion which occurred on the ITO surface during the electrodeposition. When the ITO or substrate were subjected to the cathode polarization, obvious electrochemical corrosion was observed, and some ions were changed to metal particles such as In. The composition of the glass, therefore, differed and this phenomenon caused the appearance of unknown peaks. The magnetic nanofilms may also have a stimulative effect on the crystal intensity of ITO film, for example, after the BiFeO3 films was deposited on ITO glass substrates, the intensity of diffraction peaks of ITO glass was increased [25]. Besides, this phenomenon also occurred at 40.0° in case of ITO/KIT-6/Co. Due to intense diffraction peaks of ITO/KIT-6, the diffraction peaks of metal nanofilms (such as Fe(110), Co(101), and Co(220)) were weakened to some extent.

The SEM images of ITO/KIT-6/Co and ITO/KIT-6/Fe are shown in Fig. 5. Figure 5a shows the structure of ITO/

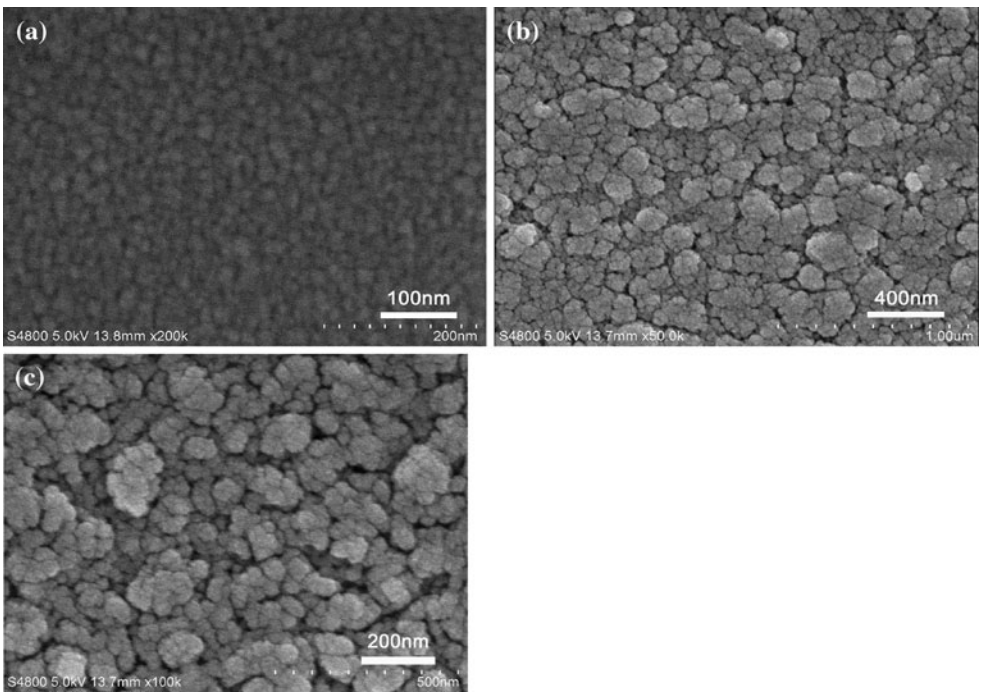

Fig. 5 SEM images of as-prepared (**a**) ITO/KIT-6/Co, (**b**) ITO/KIT-6/Co, and (**c**) ITO/KIT-6/Fe films

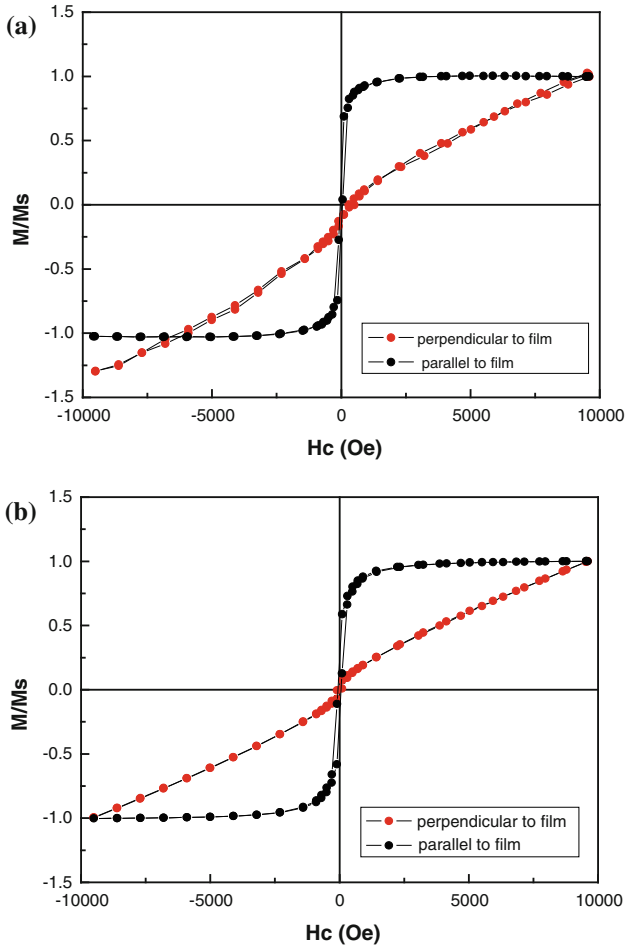

Fig. 6 Hysteresis loops of as-prepared (**a**) KIT-6/Fe and (**b**) KIT-6/Co

KIT-6/Co films obtained after electrochemical deposition of Co for 10 s. The mesoporous structure of the film was clear seen and the size of the nanowires was about 5–7 nm, which indicated the Co deposition into the mesochannels. From the Fig. 5b and c, it can be seen that the surface of the film is consisting of a number of pieces of granular film with small size which might grow along the crystal particles deposited in mesoporous of KIT-6 template. Under the disordered template and mesoporous structure, the size and shape of crystal particles grew irregularly which led to the superposition of the pieces with more than 30 nm diameter.

Magnetic measurements were performed in applied magnetic fields which were parallel and perpendicular to the film plane at room temperature. The obtained hysteresis loops of (a) KIT-6/Fe and (b) KIT-6/Co are presented in Fig. 6a, b. It is apparent from the figures that both loops exhibit the ferromagnetic behavior of Fe and Co films with the magnetic field parallel to the film. The corresponding coercivity/squarenesses were measured at 40 Oe/0.03 emu and 70 Oe/0.36 emu, respectively. On the contrary, when the external magnetic field was applied perpendicular to the film, the ferromagnetic properties behaved hardly, demonstrating the easy axis was the direction parallel to the film.

It has been widely known that when the temperature is lower than the Curie temperature, the energy to magnetic saturation of magnetic crystal varies along with different directions under the external magnetic field due to the anisotropic crystal unit volume of ferromagnetic. For each, there is a magnetic crystal orientation which requires the maximum magnetization, showing the easy magnetization direction. It should be noticed that the grains can grow along some directions because of the three-dimensional bicontinuous cubic *Ia3d* mesoporous structure. As the influence of centrifugal force of the spin coating machine increases, the nanochannels tend to arrange along the glass surface and, during the deposition, the grains grow along the channels. When the external magnetic field is parallel to the film, the magnetic film reach to saturation magnetization and shows a good ferromagnetic behavior. However, when the external magnetic field is perpendicular to the film, the ferromagnetism could not be well displayed, indicating the strong magnetic anisotropy of as-prepared Fe and Co magnetic film.

Conclusion

In this study, the mesoporous template of KIT-6 with an average pore size of 5 nm and specific surface area of 431 m^2/g was obtained by spin coating method on ITO glass. The Fe and Co magnetic nanofilms were successfully grown by electrodeposition on ITO/KIT-6 substrate. The Fe magnetic film deposited on the template grew preferentially along Fe(002) crystal direction and Co magnetic film grew along Co(101) and Co(220) crystal directions. Magnetic measurement of the hysteresis loops indicated that both the Fe and Co magnetic films possessed magnetic anisotropy and showed good ferromagnetic behavior. The coercivities at room temperature were measured at 40 and 70 Oe, respectively.

Acknowledgements This study was finically supported by Natural Science Foundation of China (No. 50701024) and Natural Science Foundation of Jiangsu Province in China (No. BK2010497).

References

1. Mor GK, Prakasam HE, Varghese OK, Shankar K, Grimes CA (2007) Nanoletters 7:2356
2. Kharisov BI, Kharissova O, Yacaman MJ (2010) Ind Eng Chem Res 49:8289
3. Nielsch K, Wehrspohn RB, Barthel J, Kirschner J, Gosele U, Ficher SF, Kronmuller H (2001) Appl Phys Lett 79:1360

4. Ross C, Chantrell R, Hwang M, Farhoud M, Saves T, Hao Y, Smith H, Ross F, Redidal M, Himphrey F (2000) Phys Rev B 62:14252
5. McGuire TR, Potter RI (1975) IEEE Trans Magn 11:1018
6. Tóth-Kadar E, Péter L, Becsei T, Tóth J, Pogány L, Tarnóczi T, Kamasa P, Bakonyi I, Láng G, Cziráki A, Schwarzacher W (2000) J Electrochem Soc 147:3311
7. Hyeon T (2003) Chem Commun 927–934
8. Lafond V, Mutin PH, Vioux A (2004) Chem Mater 16:5380–5386
9. Bearzotti A, Bertolo JM, Innocenzi P, Falcaro P, Traversa E (2004) J Eur Ceram Soc 24:1969
10. Kim TW, Kleitz F, Paul B, Ryoo R (2005) J Am Chem Soc 127:7601
11. Laha SC, Ryoo R (2003) Chem Commun 2138
12. Lv GM, Zhao R, Qian G, Qi YX, Wang XL, Suo JS (2004) J Mol Catal (China) 18:416
13. Costacurta S, Malfatti L, Innocenzi P et al (2008) Microporous Mesoporous Mater 115:338
14. Jin GQ, Guo XY (2003) Microporous Mesoporous Mater 60:207
15. Park JW, Park SS, Kim Y, Kim I, Chang SH (2008) ACS NANO 2:1137
16. Martin CR (1994) Science 266:1961
17. Hu J, Odom TW, Lieber CM (1999) Acc Chem Res 32:435
18. Choi M, Heo W, Kleitz F, Ryoo R (2003) Chem Commun 1340
19. Kim H, Cho J (2008) J Mater Chem 18:771
20. Oveisi H, Anand C, Mano A, Al-Deyab Sale\, Kalita P, Beitollahi A, Vinu A (2010) J Mater Chem 20:10120
21. Shi YF, Guo BK, Corr SA, Shi QH, Hu YS, Heier KR, Chen L, Seshadri R, Stucky DG (2009) Nano Lett 12:4215–4220
22. Brunaurr S, Emmett PH, Teller E (1938) J Am Chem Soc 60:309
23. Zhang F, Yan Y, Yang H, Meng Y, Yu C, Tu B, Zhao D (2005) J Phys Chem B 109:8723
24. Yoji D, Azusa T, Yasuhiro S (2010) Chem Commun (Camb) 46:6365
25. Liu HR, Yan BW, Wang XZ (2008) J Cryst Growth 310:2934